Journal of Sound and Vibration (2001) **245**(4), 685–699
doi:10.1006/jsvi.2000.3555, available online at http://www.idealibrary.com on IDEAL®

DYNAMICS OF FRICTION OSCILLATORS EXCITED BY A MOVING BASE AND/OR DRIVING FORCE

U. Andreaus and P. Casini

Dipartimento di Ingegneria Strutturale e Geotecnica, Facoltà di Ingegneria, Università degli Studi di Roma "La Sapienza", via Eudossiana 18, *I*-00184 *Rome, Italy. E-mail: paul.casini@uniromal.it*

(*Received* 26 *October* 1999, *and in final form* 21 *December* 2000)

The response of a single-degree-of-freedom system with dry friction under a constant velocity of the base and/or harmonic driving force is analyzed via either closed-form or numerical approaches.

The first main purpose of this paper is to investigate the influence of the base speed on the system response. To this end, in the case of a moving base with and without a harmonic driving force, as a new result, closed-form solutions are presented under the assumption of Coulomb's friction law, including a static coefficient different from the kinetic one. In more detail the existence of a critical base velocity is proved, which is the lower bound of no-stick and base-velocity-independent motions.

The second main purpose of this paper is to investigate the influence of friction modelling on the system response. To this end, the results achieved via the Coulomb's law are compared with those obtained via a particular velocity-dependent friction law; the proposed law allows the static coefficient to exponentially decay to the kinetic one, still preserving the discontinuity at null relative speed. The purpose at hand has also been accomplished by using standard numerical methods.

1. INTRODUCTION

Friction oscillators are popular subjects of analysis. Such interest can be explained in two ways. First of all, they appear in everyday life as well as in engineering systems [1–4], thus their study is of considerable practical value. In the second place, the complex dynamics exhibited by simple friction systems is a good testing bench for non-linear theories. Friction-induced vibration, chatter and squeal cause serious problems in many industrial applications, including turbine blade joints, robot joints, electric motor drives, water-lubricated bearings in ships and submarines, wheel/rail coupling of mass transit systems, machine tool/work piece systems and brake systems. These forms of vibrations are undesirable because of their detrimental effects on the operation and performance of mechanical systems. They can cause excessive wear of components, surface damage, fatigue failure, and noise [1]. As far as the theoretical motivations are concerned, one of the most important topics is the qualitative study of these systems, including the stability and bifurcation analysis and the explanation of chaotic regimes. Single-degree-of-freedom systems with dry friction have been recently studied by simulations quoted in references [2–4]. In the present paper, the motion of a single-degree-of-freedom systems with dry friction is studied via either closed-form or numerical approaches. The following standard excitations are considered: (1) moving base with constant velocity [5–10], (2) harmonic driving force [11–17] and (3) the superimposition of both [3, 12, 17–20].

0022-460X/01/340685 + 15 $35.00/0

The aim of this paper is two-fold; i.e., to study how the response of the system is affected by the base speed and by the friction law. In case (1) original closed-form solutions will be found for both transient and steady state motion, where Coulomb's friction law is assumed distinguishing the static and the kinetic coefficient. In the cases (2) and (3) a numerical investigation will be performed by assuming a particular non-smooth velocity-dependent friction law where the static coefficient exponentially decays to the kinetic one with a negative slope. In case (2) closed-form solutions are known in the literature for Coulomb's friction law [11, 13]; therefore in this paper numerical solutions will be sought in order to evaluate the influence of the negative slope on the system response. Moreover, in case (3) the influence of the base speed on the system response will be analyzed via either a closed-form or a numerical approach.

2. MODEL OF A S.D.O.F. FRICTION OSCILLATOR

2.1. EQUATION OF MOTION

The mechanical model of the friction oscillator excited by a moving base and subjected to a driving force is shown in Figure 1. A mass m is connected via a linear spring of stiffness k to a fixed support, and its position at the actual time τ with respect to the rest place $x(0) = 0$ is denoted by $x(\tau)$; in the following the prime will indicate differentiation with respect to τ. The mass can slip on a rough surface which slides with a constant velocity v_0; furthermore it may be externally excited by a harmonic driving force having an amplitude F_0 and frequency Ω: $F_t(\tau) = F_0 \cos \Omega \tau$, where the subscript "$t$" denotes the tangential direction with respect to the sliding surface. The mass is subjected to a constant compressive force $F_n \geqslant 0$ normal to the surface and the interaction between the mass and the sliding surface, which slides with respect to the mass with relative velocity $v_{rel} = v_0 - x'(\tau)$, is described by a friction force $\lambda_t(v_{rel})$. Thus, the equation of motion reads

$$m \frac{\mathrm{d}^2 x}{\mathrm{d}\tau^2} + kx - \lambda_t = F_0 \cos \Omega \tau \tag{1}$$

and it can be normalized using

$$t = \omega\tau, \qquad \omega = \sqrt{\frac{k}{m}}, \qquad \eta = \frac{\Omega}{\omega}, \qquad \dot{(\circ)} = \frac{\mathrm{d}(\circ)}{\mathrm{d}t} = \frac{1}{\omega}\frac{\mathrm{d}(\circ)}{\mathrm{d}\tau}, \qquad v_{rel} = v_0 - \omega\dot{x}, \tag{2}$$

where t denotes the non-dimensional time and the overdot indicates differentiation with respect to it.

From equations (1) and (2) it follows that

$$\ddot{x}(t) + x(t) - \frac{\lambda_t}{k} = u_s \cos \eta t, \tag{3}$$

where $u_s = F_0/k$. It should be noted that all the terms of both sides of equation (3) have the physical dimension of displacement.

The problem of modelling a friction force is still open, because the physics of dry friction is not completely understood; different models are used to reproduce various phenomena. There are two main theoretical approaches to model dry friction interfaces: the *macro-slip* and *micro-slip* approaches [1, 2, 4]. In the micro-slip approach, a relatively detailed analysis of the friction interfaces must be carried out. Generally speaking, the micro-slip approach can provide more accurate results only when the normal preload between the interfaces is

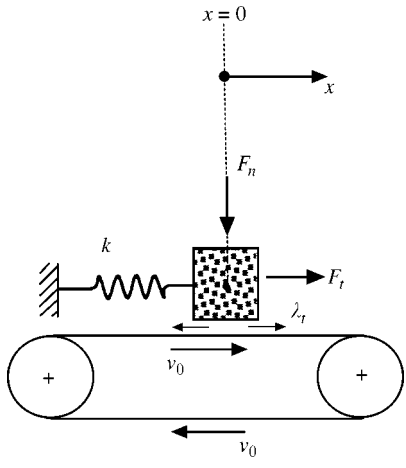

Figure 1. Model of the single-degree-of-freedom friction oscillator excited by moving base and driving force.

very high, and at the expense of a higher computational effort. In the macro-slip approach, the entire surface of the friction interface is assumed to be either slipping or stuck. We use the word macro-slip because larger-scale motion occurs when the mass velocity exceeds the transition speed from stick (micro-slip) to slip (macro-slip). Kinetic friction, i.e., the force necessary to keep sliding at a constant velocity, depends on the sliding velocity of the contact surfaces [21, 22]. With this respect, smooth [3, 14, 21] and non-smooth [3, 14, 16] velocity-dependent friction laws have been proposed in the literature. In more detail, the discontinuity at null sliding velocity is physically realistic, even though it might be not easy to be dealt with in some cases, for purposes of simulation. But the problem with the smooth model is that it allows the mass to accelerate even though the external forces on the body are less than the static friction force. Also, the need for a very steep slope around the null sliding velocity can result in very short integration time steps and numerical difficulties. The previous remarks led us to adopt non-smooth velocity dependent friction laws in the following analysis.

2.2. COULOMB'S FRICTION LAW

In this approach, the friction coefficient between the interfaces can be assumed to have two discrete values, Figure 2(a), one (μ_s) representing the static friction, the other (μ_k) the kinetic friction coefficient, or to be constant ($\mu_s = \mu_k$); in any case μ_k is independent of v_{rel}.

When the mass is at rest, the static friction will take the value necessary to balance the forces, which implies that the friction force will assume whatever value in the range $[-\mu_s F_n, \mu_s F_n]$ that is necessary to keep the contacting surfaces from sliding. Only if the magnitude of the external forces exceeds the peak force $\mu_s F_n$, will the body begin to slide. If the static friction is exceeded, the friction takes on the value of the kinetic friction, therefore the friction function $\hat{\mu}(v_{rel})$ is discontinuous and multivalued at $v_{rel} = 0$.

During the slip mode ($v_{rel} \neq 0$), the following relation

$$\frac{\lambda_t(v_{rel})}{k} = \mu_k u_0 \operatorname{sign}(v_{rel}) \tag{4}$$

holds, where $u_0 = F_n/k$.

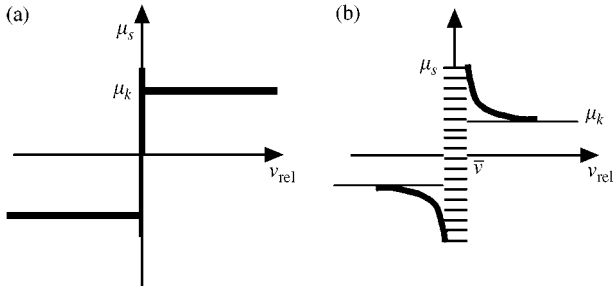

Figure 2. Velocity-dependent friction laws. (a) Non-smooth Coulomb; (b) switch model (exponential law).

During the stick mode ($v_{rel} = 0$) the friction force balances the sum of the elastic restoring force and the driving force:

$$\frac{\lambda_t(0)}{k} = x(t) - u_s \cos \eta t \tag{5}$$

and the transition from stick to slip occurs when

$$\frac{\lambda_t(0)}{k} = \mu_s u_0 \operatorname{sign}(x - u_s \cos \eta t). \tag{6}$$

That is, if the static friction force, needed to create an equilibrium with the applied forces on the mass, equals the breakaway friction force $\mu_s F_n$, the system is considered to be in transition from stick to slip.

2.3. NEGATIVE SLOPE FRICTION LAW

In the switch model [8, 9] a region of small relative velocity, shaded in Figure 2(b), is defined as $|v_{rel}| < \bar{v}$ where $\bar{v} \ll v_0$: the system is considered to be in the stick mode if the relative velocity lies inside this narrow band, which is necessary for a numerical computation.

In this paper, the switch model, as proposed in references [8, 9], is slightly improved by

(1) modelling the kinetic friction force via a particular velocity-dependent law, where the force exponentially decays with the relative speed to a residual value of friction, according to some experimental results in metal surface [21, 22];
(2) introducing a harmonic driving force as an external excitation.

By defining the state vector $(x_1, x_2, x_3) \equiv (x, \dot{x}, \eta t)$, the equations of motion governing the switch model read as follows:

Stick	*Stick to slip transition*	*Slip*
$\lvert v_{rel}\rvert \leqslant \bar{v}$ and $\lvert -x_1 + u_s \cos x_3\rvert < \frac{\mu_s F_n}{k}$,	$\lvert v_{rel}\rvert \leqslant \bar{v}$ and $\lvert -x_1 + u_s \cos x_3\rvert \geqslant \frac{\mu_s F_n}{k}$,	$\lvert v_{rel}\rvert > \bar{v}$,
$\dot{x}_1 = \frac{v_0}{\omega}$,	$\dot{x}_1 = x_2$,	$\dot{x}_1 = x_2$,
$\dot{x}_2 = \frac{v_{rel}}{\omega}$,	$\dot{x}_2 = -x_1 - \frac{\mu_s F_n}{k} \operatorname{sign}(-x_1 + u_s \cos x_3)$,	$\dot{x}_2 = -x_1 + \frac{\lambda_t}{k} \operatorname{sign}(v_{rel}) + u_s \cos x_3$,
$\dot{x}_3 = \eta$,	$\dot{x}_3 = \eta$,	$\dot{x}_3 = \eta$.

(7)

It can be observed that $\dot{x}_1$ and $\dot{x}_2$ have the physical dimension of displacement whereas $\dot{x}_3$ is a pure number. The thickness parameter $\bar{v}$ of the narrow band has to be chosen by the user. The parameter $\bar{v}$ chosen should be sufficiently small; by sufficiently small it is meant that $\bar{v}$ is small enough to have no qualitative influence on the solution. In practice, $\bar{v}$ therefore is often chosen to be much smaller than the amplitude of the mass velocity $\dot{x}_1$, or smaller than the belt velocity v_0 [9].

The kinetic friction force is modelled by the following velocity-dependent law (Figure 2(b)):

$$\lambda_t\ (v_{rel}) = -F_n\,[\mu_k + (\mu_s - \mu_k)\exp^{-\delta|v_{rel}|}]\ \mathrm{sign}\,(v_{rel}) \tag{8}$$

which exponentially decays to a residual value of friction μ_k. Parameter δ in equation (8) quantifies the descent steepness (negative slope) of the friction force.

3. MOVING BASE WITH CONSTANT VELOCITY v_0

Energy is transferred from the moving base only ($v_0 = const.$, $F_0 = 0$) to the discrete spring–mass oscillator via the friction force.

3.1. SYSTEM RESPONSE FOR COULOMB'S FRICTION LAW

For Coulomb's friction law ($\mu_s \geqslant \mu_k$) of section 2.2, closed-form solutions are determined, as a new result, for the stick mode and for the slip mode: the exact states of transition from one mode of the other are explicitly calculated and implemented as initial values for the solution of the subsequent modes. In the following, only the original results are presented, the intermediate relevant calculations and proofs having been omitted because of their cumbersomeness.

3.1.1. *Steady state motion*

For a given base speed v_0, a particular region (shaded in Figure 3(a)) in the phase plane is defined by the following inequality:

$$\Gamma_s\colon (x - \mu_k u_0)^2 + \dot{x}^2 < \frac{v_0^2}{\omega^2} \tag{9}$$

The boundary of Γ_s is a circumference having centre co-ordinates $(\mu_k u_0, 0)$ and radius $R_{\Gamma_s} = v_0/\omega$.

The initial condition state point is denoted by $P_0 = (x_0, \dot{x}_0)$. If $P_0 \in \Gamma_s$, periodic solutions, with (non-dimensional) period $T = 2\pi$, do exist in a pure slip mode: the trajectory in the phase plane is

$$\chi_s\colon (x - \mu_k u_0)^2 + \dot{x}^2 = (x_0 - \mu_k u_0)^2 + \dot{x}_0^2 \tag{10}$$

which represents a circumference having radius $R_{\chi s} = \sqrt{(x_0 - \mu_k u_0)^2 + \dot{x}_0^2}$ and centre co-ordinates $(u_0\mu_k, 0)$. It can be noted that the centre of χ_s coincides with that of Γ_s, and P_0 obviously belongs to χ_s. The mass will rest if P_0 coincides with the centre of Γ_s.

If $P_0 \notin \Gamma_s$, the transient motion is attracted by the following limit curve χ_{ss}:

$$\chi_{ss}\colon \begin{cases} \omega\dot{x} < v_0 & (x - \mu_k\mu_0)^2 + \dot{x}^2 = \frac{v_0^2}{\omega^2} + u_0^2\,(\mu_s - \mu_k)^2, \\ \omega\,\dot{x} = v_0 & u_0(2\mu_k - \mu_s) \leqslant x \leqslant u_0\mu_s\,. \end{cases} \tag{11}$$

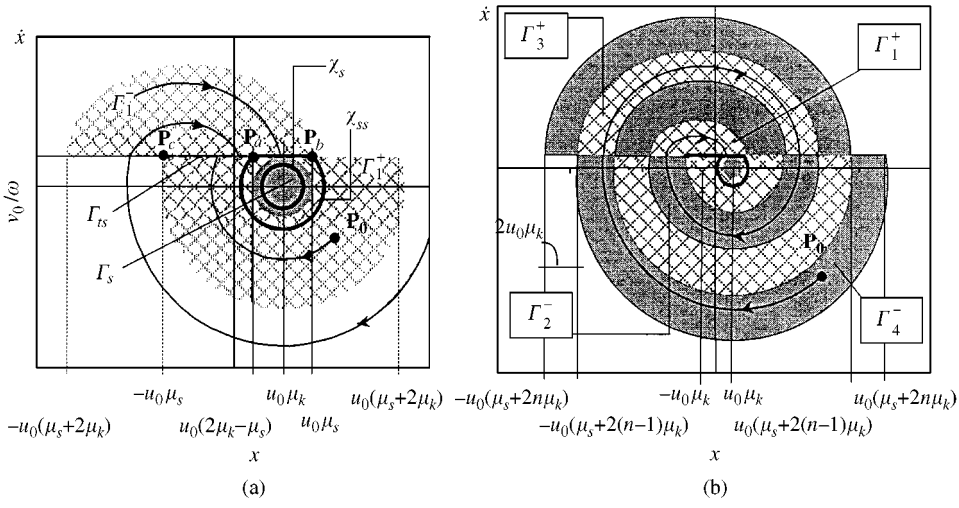

Figure 3. Phase portraits of the transient and steady state motion for general initial conditions. (a) steady state motion; (b) transient motion.

The limit curve is comprised of a circumference arc having centre co-ordinates $(u_0\,\mu_k, 0)$ and radius $R_{\chi ss} = \sqrt{u_0^2\,(\mu_s - \mu_k)^2 + v_0^2{}^*\omega^2}$ and of a straight segment beginning at P_a, ending at P_b, and hence having a length $2u_0\,(\mu_s - \mu_k)$. It is worth noting that the displacements of point P_a and P_b, i.e., the extreme points of the steady stick motion, do not depend on v_0; the (non-dimensional) duration of the steady stick motion is

$$\Delta t_{st} = 2u_0\,(\mu_s - \mu_k)\,\omega/v_0. \tag{12}$$

With reference to Figure 3(a), t_b is the time at which P_b is attained for the first time; in order to evaluate the (non-dimensional) duration Δt_{sl} of the steady slip motion, equation (3) and (4) relative to the slip mode is solved for the initial condition $x = x(t_b) = u_0\mu_s$ and $\dot{x} = \dot{x}(t_b) = v_0/\omega$ and the desired value

$$\Delta t_{sl} = \arccos\frac{v_0^2/\omega^2 - u_0^2\,(\mu_s - \mu_k)^2}{v_0^2/\omega^2 + u_0^2\,(\mu_s - \mu_k)^2} \tag{13}$$

is calculated by imposing the condition $\dot{x}(t_b + \Delta t_{sl}) = v_0/\omega$. Also in this case the response is periodic with (non-dimensional) period $T = \Delta t_{st} + \Delta t_{sl}$.

3.1.2. *Influence of the base speed on the steady state response*

In order to analyze the influence of the base speed on the steady state response, the lessening sign in inequality (9) is substituted by the equality sign and the equation so obtained is solved in terms of v_0 for fixed initial conditions $(x_0, \dot{x}_0)$; therefore, the following critical value for the base speed is yielded, Figures 4(a) and (b):

$$v_0^* = \omega\sqrt{(x_0 - \mu_k u_0)^2 + \dot{x}_0^2} \tag{14}$$

such that $\partial\Gamma_s$ passes through $P_0 = (x_0, \dot{x}_0)$. In other words, if the definition of Γ_s given above is recalled, the physical meaning of the critical value v_0^* does appear: if the

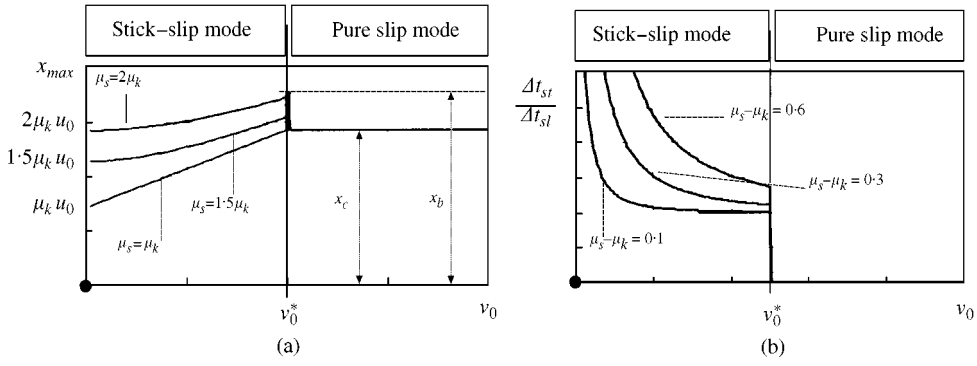

Figure 4. Influence of base speed on the steady state response for fixed μ_k and P_0 (*Coulomb's friction law*). (a) Influence on displacement amplitude; (b) influence on the duration of the stick mode.

base velocity v_0 is larger than v_0^* non-stick and base-velocity-independent motions are exhibited.

(1) If $v_0 < v_0^*$ (i.e., $P_0 \notin \Gamma_s$) the maximum displacement depends on v_0 according to the monotonically increasing relationship $x_{max} = \mu_k u_0 + \sqrt{v_0^2/\omega^2 + u_0^2(\mu_s - \mu_k)^2}$ which becomes linear for $\mu_s = \mu_k$. The durations Δt_{st}, Δt_{sl} of the steady stick mode and of the steady slip mode are given by equations (12) and (13); thus the period is $T = \Delta t_{st} + \Delta t_{sl}$.
(2) If $v_0 = v_0^*$ (i.e., $P_0 \notin \Gamma_s$) transition between pure sliding and stick–slip motion takes place and the maximum displacement is $x_b = \mu_k u_0 + \sqrt{v_0^{*2}/\omega^2 + u_0^2(\mu_s - \mu_k)^2}$.
(3) If $v_0 > v_0^*$ (i.e, $P_0 \in \Gamma_s$) the maximum displacement $x_c = \mu_k u_0 + \sqrt{(x_0 - \mu_k u_0)^2 + \dot{x}_0^2} \leqslant x_b$ is independent of v_0 and the duration of the steady stick mode is zero (i.e., pure slip mode); the period becomes independent of v_0 and equal to 2π.

Thus, as v_0 increases up to v_0^*, x_{max} increases up to x_b, then it abruptly falls to x_c, whereas in the case of $\mu_s = \mu_k$, $x_{max} = \mu_k u_0 + v_0/\omega$ and attains x_c without any jump.

The above results can be particularized to the case of $\mu_s = \mu_k$: in more detail, it should be noted that χ_{ss} coincides with $\partial\Gamma_s$, the steady stick motion reduces to one point and the (non-dimensional) period of the steady state motion is in any case independent of v_0 and equal to 2π.

3.1.3. *Transient motion*

If $P_0 \notin \Gamma_s$, a transient motion is exhibited which is comprised of a finite integer number $n \geqslant 0$ of sliding modes and a final stick mode.

A straight segment $P_c P_b$ has been found

$$\Gamma_{ts}: \omega\dot{x} = v_0 \qquad -u_0\mu_s \leqslant x \leqslant u_0\mu_s \tag{15}$$

such that if $P_0 \in \Gamma_{ts}$ no transient slip modes are exhibited ($n = 0$) and the transient motion is constituted uniquely by a stick mode coincident with the segment $P_0 P_b \in \Gamma_{ts}$.

If $P_0 \notin \Gamma_{ts}$, $n > 0$ and for a fixed "n", two particular regions have been found (Figure 3(b))

$$\Gamma_n^+ := \gamma_n^+ \setminus \gamma_{n-1}^+$$
$$\Gamma_n^- := \gamma_n^- \setminus \gamma_{n-1}^- \tag{16}$$

where the backslash (\ ) denotes set subtraction. The regions γ_n^+ and γ_n^- are defined as follows:

$$\gamma_n^- : \begin{cases} \omega\dot{x} < v_0, & (x-\mu_k u_0)^2 + \dot{x}^2 \leqslant \dfrac{v_0^2}{\omega^2} + u_0^2\,[\mu_s + (2n-1)\mu_k]^2 \\ \omega\,\dot{x} = v_0, & u_0[\mu_s + (2n-1)\mu_k] \leqslant x \leqslant u_0(\mu_s + 2n\mu_k) \end{cases} \tag{17}$$

$$\gamma_n^+ : \begin{cases} \omega\dot{x} > v_0, & (x+\mu_k u_0)^2 + \dot{x}^2 \leqslant \dfrac{v_0^2}{\omega^2} + u_0^2\,[\mu_s + (2n-1)\mu_k]^2 \\ \omega\,\dot{x} = v_0, & -u_0(\mu_s + 2n\mu_k) \leqslant x \leqslant -u_0\,[\mu_s + (2n-1)\mu_k] \end{cases} \tag{18}$$

The plane regions γ_n^+ and γ_n^- are circumferential bowls of centres $(\mp\mu_k u_0, 0)$ and radius $\sqrt{v_0^2/\omega^2 + u_0^2\,[\mu_s + (2n-1)\mu_k]}$.

Starting from either $P_0 \in \Gamma_n^+$ or $P_0 \in \Gamma_n^-$, the transient motion is constituted by "n" subsequent slip modes and one stick mode: the trajectory will belong alternatively to the sequence

$$\underbrace{\Gamma_n^{\pm} \to \Gamma_{n-1}^{\mp} \to \Gamma_{n-2}^{\pm} \to \cdots}_{\text{"}n\text{" transient slip modes}} \to \underbrace{\Gamma_{ts}}_{\text{transient stick mode}} \to \text{limit curve } \chi_{ss}.$$

Each slip trajectory is defined by a circumference arc and the transition from one to another occurs at the sign inversion of the relative speed. The convergence of the solution of the transient slip modes to the transient stick mode and then to the limit curve has been verified by matching with each other the subsequent regular paths of motion. In more detail, as far as the sequence of transient slip modes are concerned, each mode is governed by the equation of motion (equation (3)) and by the friction force (equation (4)) and the transition from one mode to the subsequent one is ruled by null relative velocity and external force exceeding the breakaway friction force. The transition from the last transient slip mode to the transient stick mode is decided by null relative velocity and external force getting smaller than the breakaway friction force; so far, a transient stick mode of the finite duration takes place, which ends in a system state belonging to the limit curve, as soon as equation (6) is satisfied.

3.2. SYSTEM RESPONSE FOR NEGATIVE SLOPE FRICTION LAW

The aim of this section is twofold: (1) to evaluate the influence of the base speed on the system response for different friction laws, namely Coulomb's law and negative slope law, and (2) to perform a sensitivity analysis of qualitative properties of the obtained numerical solutions as far as the descent steepness of the negative slope law, governed by parameter δ, is concerned. The analysis of the system response where the negative slope law is adopted to simulate friction force requires the use of the switch model of the section 2.3. It should be noted that if the driving force is missing ($u_s = 0$) the governing equations read as follows:

Stick	*Stick to slip transition*	*Slip*
$\dot{x}_1 = \dfrac{v_0}{\omega},$	$\dot{x}_1 = x_2,$	$\dot{x}_1 = x_2,$
$\dot{x}_2 = \dfrac{v_{rel}}{\omega},$	$\dot{x}_2 = -x_1 - \dfrac{\mu_s F_n}{k}\,\mathrm{sign}(-x_1),$	$\dot{x}_2 = -x_1 + \dfrac{\lambda_t(v_{rel})}{k},$

(19)

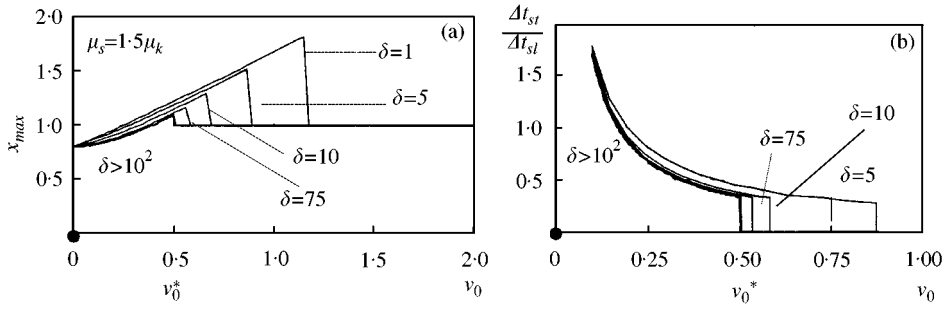

Figure 5. Influence on base speed on the steady state response for fixed μ_k and $P_0 = (0, 0)$ (*Negative slope law* with $\omega = 1$ rad/s, $\mu_s = 1{\cdot}0$). (a) Influence on displacement amplitude; (b) influence on the duration of the stick mode.

where λ_t is still given by equation (8). The numerical solutions of equations (19) have been obtained via the Runge–Kutta–Fehlberg integration algorithm [23], taking a tolerance much smaller than $\bar{v}$ [9].

With reference to the first aim, even in the case of the negative slope law, a critical velocity v_0^* does exist, which in addition depends on δ, besides x_0, $\dot{x}_0$ and ω, as it happens for Coulomb's oscillator, equation (14). The function $v_0^*(x_0, \dot{x}_0, \delta, \omega)$ is unfortunately unknown in closed form; thus Figures 5(a) and (b) refer to the case $\omega = 1$ and to natural initial conditions, whereas the dependence of the critical base speed on the parameter δ is shown in numerical form.

Figure 4(a) (Coulomb's law) should be compared with Figure 5(a) (negative slope law), which shows the dependence of x_{max} on v_0 for different values of decaying coefficient δ, equation (8). In more detail, the critical velocity v_0^* increases as the module of the negative slope reduces ($\delta \to 0$), and when the base speed exceeds this critical value, x_{max} abruptly falls to the value $x_c = \mu_k u_0 + \sqrt{(x_0 - \mu_k u_0)^2 + \dot{x}_0^2}$. For different values of δ, an analogous comparison between Figures 5(b) and 4(b) can be done as far as the dependence on v_0 of the durations of the steady stick and slip modes is concerned.

The comparison of the system responses for Coulomb's law (Figure 6(a)) and negative slope (Figure 6(b)) in the phase plane for natural initial conditions shows that, for the negative slope, the length of the stick mode increases as the base velocity increases, whereas in the case of Coulomb's friction law it is independent of v_0 and is given by $2u_0(\mu_s - \mu_k)$, as already shown in section 3.1.

4. THE PRESENCE OF DRIVING FORCE

4.1. STICK–SLIP TRANSITIONS

As an aid in describing and understanding non-linear systems, one can introduce maps between different sections of the state space. A convenient way to study non-smooth oscillators is a map P relating one discontinuity to the next. The structure of the three-dimensional phase space for the friction oscillator motivates a natural choice [3, 13]. The basic dynamics of the friction oscillator can be described by a "stick–slip transition" map $P_F(\phi)$, where ϕ is defined by $\phi = x_3 \bmod 2\pi/\eta$. This map relates the phase ϕ_i where the velocity $x_{2,i} = v_0$, at a transition point from stick to slip, to the phase ϕ_{i+1} of the next stick–slip transition. In general the map works on Poincarè section:

$$\Sigma_F = \{(x_1, x_2; \phi) \,|\, x_2 = v_0, \qquad |-x_1 + u_s \cos\phi| = \mu_s u_0\} \tag{20}$$

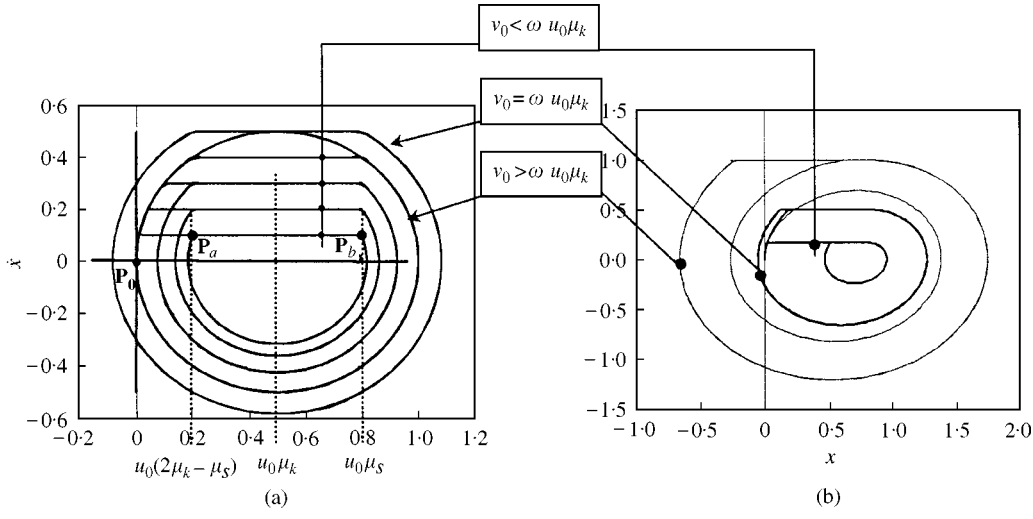

Figure 6. Phase portraits of the transient and steady state motion for natural initial conditions. (a) Coulomb's friction law ($\mu_s > \mu_k$); (b) negative slope ($\mu_s = 1{\cdot}0$, $\mu_k = 0{\cdot}8$, $\delta = 1$ s/m and $v_0 = 0{\cdot}0$–$1{\cdot}00$ m/s).

which represents the sticking region, so that the system dynamics is reduced to dimension one. The stick–slip transition map reads as follows:

$$P_F: \begin{cases} \Sigma_F & \to & \Sigma_F \\ \phi_i & \to & \phi_{i+1}. \end{cases} \tag{21}$$

So, by means of the map P_F one can study the system dynamics of the investigated non-smooth systems. Unfortunately, P_F cannot be given explicitly [13] and in the following it will be obtained via the Runge–Kutta–Fehlberg integration algorithm [23]. Let $\phi_0 \in \Sigma_F$ be the state of the first transition of the orbit. The map P_F allows us to determine the countable set of the next transition state $\phi_i \in \Sigma_F$:

$$\phi_i = P_F^i(\phi_0), \qquad P_F^i = \underbrace{P_F \circ P_F \circ \cdots \circ P_F}_{i \text{ times}}. \tag{22}$$

A *j-transition periodic* motion is simply defined by the equation

$$P_F^j(\phi_0) - \phi_0 = 0. \tag{23}$$

In other terms, a j-transition periodic orbit is completely defined as the fixed point of the map P_F^j.

4.2. DRIVING FORCE AND FIXED BASE ($F_0 \neq 0$, $v_0 = 0$)

The model adopted to simulate the friction characteristic can affect the response of the friction oscillator, both quantitatively and qualitatively, namely the number of stops per cycle, the maximum amplitude of displacement and velocity, and the period of steady state motion.

As a sample application, Figures 7(a) and (b) allow one to compare, respectively, displacement and velocity time-histories for a Coulomb oscillator with the negative slope

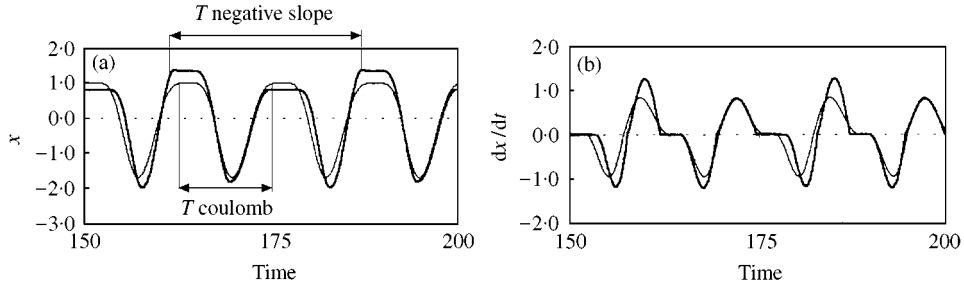

Figure 7. Comparison between Coulomb's (thin line) and negative slope ($\delta = 1$ s/m, thick line) laws ($\mu_s = 0{\cdot}5$, $\mu_k = 0{\cdot}1$, $\eta = 0{\cdot}1$, $u_s = 1{\cdot}0$ m). (a) Displacement time-histories; (b) velocity time-histories.

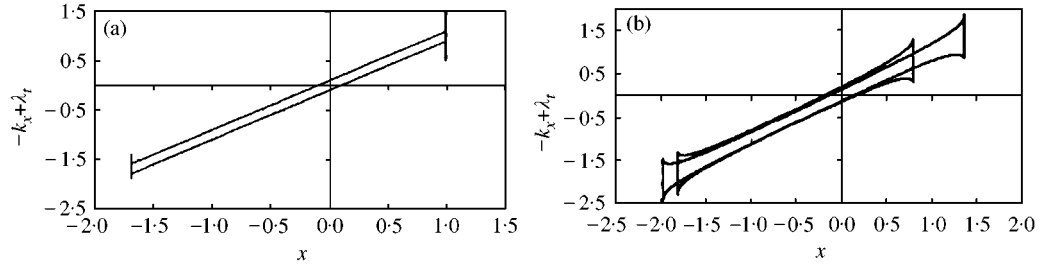

Figure 8. External force acting on the mass in terms of displacement ($\mu_s = 0{\cdot}5$, $\mu_k = 0{\cdot}1$, $\eta = 0{\cdot}1$, $u_s = 1{\cdot}0$ m). (a) Coulomb's law; (b) negative slope law ($\delta = 1$ s/m).

oscillator of section 2.3. It can be of some interest to observe that the negative slope oscillator steady response has a period which is twice that of the Coulomb oscillator, while two and one stop per cycle are exhibited, respectively, in the former and in the latter case. Coulomb oscillator and negative slope oscillator can also be compared in terms of energy dissipated during one response cycle. To this end, with reference to the cases studied in Figure 7, a diagram has been traced by plotting the external force (i.e., the sum of frictional and restoring forces) acting on the mass in terms of displacement. In this way the enclosed area measures the energy dissipated by friction. This is done in Figures 8(a) and (b) referring to the hysteretic behaviour of Coulomb and negative slope oscillators respectively.

4.3. DRIVING FORCE AND MOVING BASE ($F_0 \neq 0$, $v_0 \neq 0$)

The combined effect of moving base and driving force determines the existence, for each value of the frequency ratio, of a critical value v_0^* of the base speed above which the response is not affected by v_0, as already observed in section 3.

In the case of Coulomb friction, this critical value has been found in closed form (solid line in Figure 9) as illustrated in the following. For any initial condition, assuming $v_0 \neq 0$ (e.g., $v_0 > 0$, without loss of generalities) causes the first regular path of the transient motion to be characterized by the slip mode, with the exception of the trivial case ($|x(0) - u_s| \leqslant \mu_s u_0$, $\dot{x}(0) = v_0/\omega$) which determines an initial stick mode. The equation of motion (3) with the friction force (equation (4)) admits a closed-form solution in terms of velocity:

$$\dot{x}(t) = \frac{\dot{x}_0(\eta^2 - 1)\cos t - [u_s + (\eta^2 - 1)(x_0 - \mu_k u_0)]\sin(t) + u_s \eta \sin \eta t}{\eta^2 - 1}. \tag{24}$$

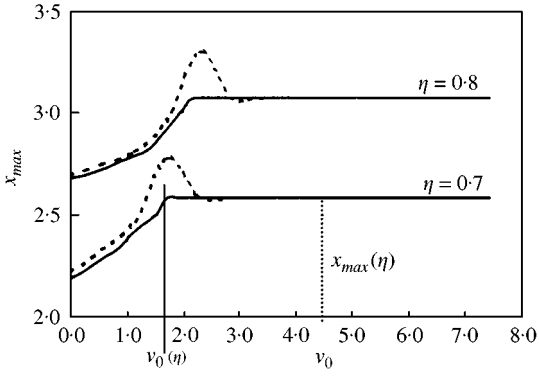

Figure 9. Influence of base speed on displacement amplitude for Coulomb's (solid lines) and negative slope (dashed lines) laws for $\mu_s = 1{\cdot}0$, $\mu_k = 0{\cdot}8$, $\delta = 1$ s/m, $u_s = 1{\cdot}0$ m.

The inequality

$$\dot{x}(t) < \frac{v_0}{\omega} \; \forall t \tag{25}$$

avoids slip–stick transitions and allows the oscillator to indefinitely remain in the slip mode. In fact inequality (25) prescribes the relative velocity, given by equation $(2)_5$, to be always larger than zero; whereas a stick–slip transition occurs when the relative velocity gets a null value.

In order to investigate the consequences of equation (24) and to make their interpretation easier, the study is herein limited to the forced response which, yet being a particular case, is widely encountered in practical applications. This end is achieved by introducing in equation (24) the particular initial conditions

$$x(0) = \mu_k u_0 + \frac{u_s}{1 - \eta^2}, \qquad \dot{x}(0) = 0 \tag{26}$$

which anneal the general solution; therefore, equation (24) reads as follows:

$$\dot{x}\,(t) = \frac{u_s \eta}{|1 - \eta^2|} \sin \eta t \tag{27}$$

and inequality (25) becomes

$$\dot{x}\,(t) = \frac{u_s \eta}{|1 - \eta^2|} \sin \eta t < \frac{v_0}{\omega}. \tag{28}$$

Thus, obviously, if it happens that

$$v_0 > \omega \frac{u_s \eta}{|1 - \eta^2|} \tag{29}$$

inequality (28) does hold for every time t. Defining

$$v_0^*(\eta, \omega) := \omega \frac{u_s \eta}{|1 - \eta^2|} \tag{30}$$

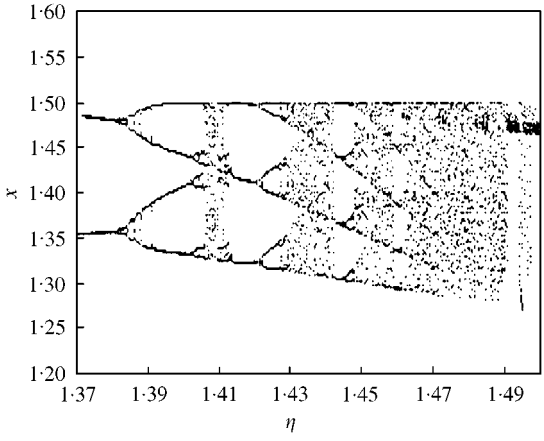

Figure 10. Period-doubling cascade for $v_0 = 0{\cdot}5$ m/s, $\mu_s = 1{\cdot}0$, $\mu_k = 0{\cdot}8$, $\delta = 1$ s/m and $u_s = 0{\cdot}5$ m.

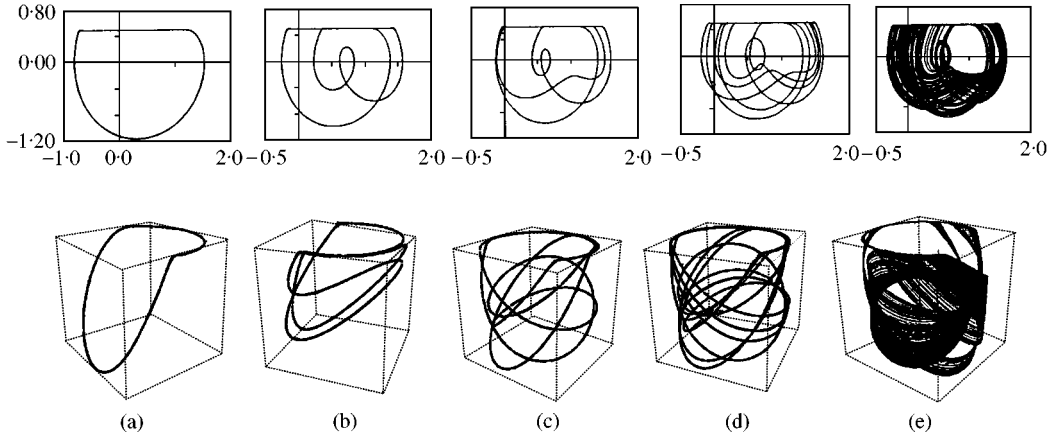

Figure 11. Different types of responses. (a) One-transition periodic solution ($\eta = 1{\cdot}250$); (b) two-transition periodic solution ($\eta = 1{\cdot}370$); (c) three-transition periodic solution ($\eta = 1{\cdot}415$); (d) six-transition periodic solution ($\eta = 1{\cdot}424$); (e) chaotic behaviour ($\eta = 1.431$).

shows the explicit dependence of the critical relative velocity on η and ω (linearly) and the implicit dependence on the initial conditions (26). In other words, if v_0 is larger than v_0^*, then $\dot{x}(t)$ is always smaller than v_0/ω and therefore, since no sign inversion of the relative speed can occur, the response is independent of belt speed.

By using the negative slope model, we have numerically found that a critical base velocity $v_0^*(\eta, \delta, x_0, \dot{x}_0)$ still exists and increases as $\delta \to 0$ and as $\eta \to 1$; the initial conditions (26) and $\omega = 1$ yield the numerical results represented by the dashed lines in Figure 9.

In the bifurcation diagram of Figure 10 the displacement characterizing the transition from stick to slip is plotted as a function of the bifurcation parameter η, for the friction characteristic of Figure 2(b). One can distinguish one-periodic and higher-periodic solutions. For large values of η, period-doubling cascades have been found, which indicate a route to chaotic motion. For clarity, once again the phase plane plots of one-, two-, three- and six-transition-periodic solutions, as well as of chaotic motion are shown in Figure 11 (top). The corresponding trajectories in the three-dimensional state space are illustrated at the bottom level of the previously mentioned Figure 11.

5. CONCLUDING REMARKS

The motion of a s.d.o.f. friction oscillator has been analyzed under (1) constant velocity imposed to the base, (2) harmonic driving force and (3) their combination.

As a new result, closed-form solutions have been found in the case of a moving base with Coulomb's friction law. The steady state motion is characterized by either a pure slip mode or a stick–slip mode: the trajectories equations have been given for either cases in the phase plane as well as the conditions to be satisfied by the initial state in order to avoid noising stick–slip vibrations. The influence of the base speed both on the amplitude of displacement and on the stick mode duration has been examined; in particular, a critical value of the base speed (depending on the initial conditions and on the kinetic friction) has been found in a closed form above which the oscillator response does not depend on the base velocity and the stick–slip vibrations disappear. The transient motion has been studied to find the conditions which must be satisfied by the initial state in order to determine the sequence of pure slip modes and the unique stick mode preceding the steady state. The influence of the friction model on the system response has been analyzed by using a "negative slope" friction law and the existence of a critical value of the base speed has been demonstrated also in this case, which increases as the descent of the decaying branch becomes less steep.

In the case of a harmonic driving force the influence of the friction model on the steady response has been studied by comparing the results obtained by either the Coulomb's or the negative slope laws: in the latter case the period and the number of stops per cycle can significantly increase.

Also in the case of a combined moving base and driving force with Coulomb's law, a critical value of the base speed has been found in the closed form for each value of the frequency ratio and for given initial conditions; as in the case of the exclusive presence of the moving base, the oscillator response is independent of the base velocity whenever it exceeds the critical value. It has been recognized that, in the presence of a negative slope, this critical velocity shifts towards larger values as the slope gets less steep. For a response depending on base velocity, period-doubling cascades as well as n-periodic solutions exhibiting more than one cycle and chaotic motions are exhibited.

REFERENCES

1. R. Ibrahim 1994 *Applied Mechanics Review* **47**, 209–226. Friction induced vibration, chatter, squeal and chaos Part I: mechanics of contact and friction.
2. R. Ibrahim 1994 *Applied Mechanics Review* **47**, 227–253. Friction induced vibration, chatter, squeal and chaos Part II: dynamics and modelling.
3. K. Popp, N. Hinrichs and M. Oestreich 1996 in *Dynamics with friction* (A. Guran, F. Pfeiffer, and K. Popp, editors), London: World Scientific. Analysis of a self-excited friction oscillator with external excitation, pp. 1–35.
4. B. Feeny, A. Guran, N. Hinrichs and K. Popp 1998 *Applied Mechanics Review* **51**, 321–341. A historical review on dry friction and stick-slip phenomena.
5. E. Rabinowicz 1958 *Proceedings of Physical Society London* **71**, 668–675. The intrinsic variables affecting the stick–slip process.
6. B. Armstrong-Helouvry, P. Dupont and C. Canudas de Wit 1994 *Automatica* **30**, 1083–1131. A survey of models analysis tools and compensation methods for the control of machines with friction.
7. J. Sikora 1991 *ZAMM Zeitschrift für Angewandte Mathematik und Mechanik* **71**, 63–66. On the influence of viscous damping on the properties of mechanical system with friction.
8. R. I. Leine, D. H. Van Campen, A. De Kraker and L. Van Den Steen 1998 *Nonlinear Dynamics* **16**, 41–54. Stick–slip vibration induced by alternate friction models.
9. R. I. Leine 2000 *Ph.D. Thesis*, *Technische Universiteit Eindhoven*. Bifurcations in discontinuous mechanical systems of Filippov-type.

10. U. ANDREAUS and P. CASINI 2001 *International Journal of Nonlinear Mechanics* **37**, 117–133. Friction oscillators excited by moving base and colliding with rigid or deformable obstacle.
11. J. P. DEN HARTOG 1931 *Transactions American Society of Mechanical Engineers* **53**, 107–115. Forced vibrations with combined Coulomb and viscous friction.
12. E. MARUI and S. KATO 1984 *American Society of Mechanical Engineers Journal of Dynamic Systems, Measurement and Control* **106**, 280–285. Forced vibration of a base-excited SDOF system with Coulomb friction.
13. S. H. SHAW 1986 *Journal of Sound and Vibration* **108**, 305–325. On the dynamic response of a system with dry friction.
14. N. MAKRIS and M. C. CONSTANTINOU 1991 *Mechanics of Structures and Machines* **19**, 477–500. Analysis of motion resisted by friction. I. Constant Coulomb and linear/Coulomb friction.
15. N. MAKRIS and M. C. CONSTANTINOU 1991 *Mechanics of Structures and Machines* **19**, 501–526. Analysis of motion resisted by friction. II. Velocity-dependent friction.
16. S. NATSIAVAS 1998 *Journal of Sound and Vibration* **217**, 507–522. Stability of piece-wise linear oscillators with viscous and dry friction damping.
17. U. ANDREAUS and P. CASINI 2001 *Journal of Structures and Machines* **29**, 177–198. Forced motion of friction oscillators limited by a rigid or deformable obstacle.
18. K. POPP and P. STELTER 1989 *IUTAM Symposium on Nonlinear Dynamics in Engineering Systems, Stuttgart*. Nonlinear oscillation of structures induced by dry friction.
19. S. NARAYANAN and K. JAYARAMAN 1991 *Journal of Sound and Vibration* **146**, 17–34. Chaotic vibration in a nonlinear oscillator with Coulomb friction.
20. A. OSSOWSKI 1999 *Journal of Sound and Vibration* **222**, 521–530. Asymptotic behaviour of an oscillator excited by dry friction forces.
21. J. T. ODEN and J. A. C. MARTINS 1985 *Computer Methods in Applied Mechanics Engineering* **52**, 527–634. Models and computational methods for dynamic friction phenomena.
22. J. H. WANG 1996 in *Dynamics with friction* (A Guran, F. Pfeiffer and K. Popp, editors), London: World Scientific. Design of a friction damper of control vibration of turbine blades, pp. 169–195.
23. C. F. GERALD and P. O. WHEATLEY 1994 *Applied Numerical Analysis*. Reading, MA: Addison-Wesley.